

Full paper / Mémoire

# Preparation and catalytic activity of nickel–manganese oxide catalysts in the reaction of partial oxidation of methane

Maha Hadj-Sadok Ouaguenouni <sup>a,\*</sup>, Amel Benadda <sup>a</sup>, Alain Kiennemann <sup>b</sup>,  
Akila Barama <sup>a</sup>

<sup>a</sup> *Laboratoire de chimie du gaz naturel, Faculté de chimie, USTHB, BP32 El Alia, Bab Ezzouar, 16111 Alger, Algeria*

<sup>b</sup> *ECPM-LMSPC UMR, CNRS 7515, 25, rue Bacquerel, 67087 Strasbourg, France*

Received 5 May 2008; accepted after revision 10 December 2008

Available online 10 February 2009

## Abstract

Nickel–manganese mixed oxides were prepared with sol–gel and coprecipitation methods. The characterization of the different samples was made by XRD, TPR, FT-IR and Raman spectroscopies. NiMn<sub>2</sub>O<sub>4</sub> spinel was obtained at a calcination temperature of 900 °C; the solids calcined at 750 °C give in addition to the spinel phase, an ilmenite phase (NiMnO<sub>3</sub>) and a Mn<sub>2</sub>O<sub>3</sub> phase. Preliminary reactivity results of partial oxidation of methane on NiMn<sub>2</sub>O<sub>4</sub> and sub-stoichiometric Ni<sub>x</sub>Mn<sub>3-x</sub>O<sub>4</sub> are given. The catalysts calcined at 900 °C presented the best methane conversion at 700 °C. The solid containing the ilmenite phase leads to a high CO<sub>2</sub> selectivity revealing a good activity towards the complete oxidation of methane. **To cite this article:** *M. Hadj-Sadok Ouaguenouni et al., C. R. Chimie 12 (2009).*

© 2008 Published by Elsevier Masson SAS on behalf of Académie des sciences.

## Résumé

Les oxydes mixtes nickel–manganese ont été préparés par deux méthodes différentes : coprécipitation et la méthode sol–gel. Les différents solides préparés ont été caractérisés par DRX, TPR, FT-IR et spectroscopie Raman. Une structure spinelle pure a été obtenue après calcination à 900 °C ; les solides calcinés à 750 °C donnent lieu, en plus de la phase spinelle, à deux phases supplémentaires NiMnO<sub>3</sub> et Mn<sub>2</sub>O<sub>3</sub>. NiMn<sub>2</sub>O<sub>4</sub> et les solides sous-stoechiométriques Ni<sub>x</sub>Mn<sub>3-x</sub>O<sub>4</sub> ont été testés dans la réaction d'oxydation partielle du méthane. Les catalyseurs calcinés à 900 °C conduisent à la meilleure conversion du méthane. Une sélectivité importante en CO<sub>2</sub> a été obtenue avec le solide contenant la phase ilménite révélant ainsi une bonne activité dans la réaction d'oxydation complète du méthane. **Pour citer cet article :** *M. Hadj-Sadok Ouaguenouni et al., C. R. Chimie 12 (2009).*

© 2008 Published by Elsevier Masson SAS on behalf of Académie des sciences.

\* Corresponding author.

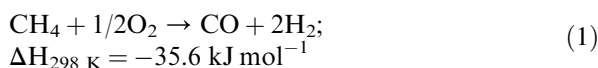
*E-mail address:* [hsomaha@yahoo.fr](mailto:hsomaha@yahoo.fr) (M. Hadj-Sadok Ouaguenouni).

*Keywords:* Manganese, nickel, oxides; Coprecipitation; Sol–gel; Partial oxidation of methane

*Mots-clés :* Manganese, nickel, oxydes ; Coprécipitation ; Sol–gel ; Oxydation Partielle du méthane

## 1. Introduction

Partial oxidation of methane (POM) (reaction (1)), to produce syngas, is a process that is still very much studied for many advantages compared to steam reforming of CH<sub>4</sub>. It is an exothermic reaction and produces syngas with H<sub>2</sub>/CO ratio of about 2 which is ideal for further methanol and Fischer–Tropsch syntheses [1–4].



Although precious metals, such as Ru, Rh, Ir and Pt, have been employed successfully for this reaction in terms of activity and selectivity [5,6], the high cost and limited availability of the noble metals restrict their applications. On the other hand, nickel catalysts have been widely used due to their high activity and low cost. However, most commercial nickel-based catalysts suffer deactivation due to sintering and carbon deposition during operation [7,8]. Catalysts that are more resistant to deactivation have been developed by nickel insertion into a well-defined structure, such as perovskites, spinels, ..., the strong interaction existing within the structure leads to the formation of small nickel particles upon the reduction of the catalyst: which resulted in a high dispersion of the active species [9,10]. On the other hand, nickel catalysts with various additives have been reported, and other transition-metal oxides have proved to be active in the catalytic oxidation of hydrocarbons. The best catalytic performance was achieved with 3d-transition-metal oxides composed of cations in their higher oxidation state. Furthermore, it has been shown that the Cu, Co and Ni mixed oxides with a spinel-type structure are more active than the single oxides [11,12].

Mixed nickel–manganese oxides adapt two types of crystal structure: spinel (NiMn<sub>2</sub>O<sub>4</sub>) and ilmenite (NiMnO<sub>3</sub>). In the spinel structure, Ni<sup>2+</sup>, Mn<sup>2+</sup>, Mn<sup>3+</sup> and Mn<sup>4+</sup> ions can coexist and are distributed among the tetrahedral and octahedral spinel sites, whereas in the ilmenite structure both Ni<sup>2+</sup> and Mn<sup>4+</sup> are in octahedral position.

In this study, we report the preparation of NiMn<sub>2</sub>O<sub>4</sub> using coprecipitation and sol–gel methods. Preliminary reactivity results of methane partial oxidation will

be given, so that the activity and the structure of catalysts could be correlated.

## 2. Experimental

### 2.1. Catalyst preparation

#### 2.1.1. Coprecipitation method

Nickel–manganese mixed oxides were prepared from carbonate precursors [13]. The mixed appropriate amounts of manganese and nickel nitrate solutions with Ni/Mn = 1/2 were added into a well-stirred container containing sodium bicarbonate solution at room temperature. The obtained solid was dried at 60 °C and calcined at 750 and 900 °C for 12 h in air, the heating rate was 5 °C min<sup>-1</sup>. The solids prepared by the coprecipitation method and calcined at 750 and 900 °C will be denoted, respectively, as CP750 and CP900.

Mn<sub>3</sub>O<sub>4</sub> and the sub-stoichiometric Ni<sub>x</sub>Mn<sub>3-x</sub>O<sub>4</sub> ( $x = 0.2, 0.6, 0.8$ ) were prepared following the same protocol and then calcined in air for 12 h at 900 °C. These solids will be denoted as CP- $x$ -900, where  $x$  stands for the stoichiometric nickel content.

#### 2.1.2. Sol–gel method

The nickel–manganese mixed oxide was also prepared by a pseudo-sol–gel method based on the thermal decomposition of propionate precursors [14]. The starting materials were nickel(II) acetate hydrate and manganese(II) acetate hydrate. The salts were dissolved separately in boiling propionic acid with a concentration of 0.12 mol l<sup>-1</sup> in cation. The two boiling solutions were then mixed so as to have Ni:Mn = 1:2 and the solvent was evaporated under continuous stirring until a resin was obtained. The resin was directly calcined in air at 750 and 900 °C for 12 h. The solids prepared by the sol–gel method will be denoted as SG750 and SG900, where 750 and 900 stand for the calcination temperatures.

### 2.2. Technique characterization

The atomic ratio of metals was checked by atomic absorption spectroscopy. X-ray diffraction experiments were performed on a D500 Siemens diffractometer

using the Cu K $\alpha$  radiation ( $\lambda = 0.15406$  nm). The data were collected at  $0.03^\circ$  with a counting time of 2 s per step, in the ( $2\theta$ ) range from  $20^\circ$  to  $80^\circ$ . The crystalline phases were identified by reference to the powder diffraction data (JCPDS) with the use of standard spectra software. Fourier-transform infrared (FT-IR) spectra were recorded using a Shimadzu 8400 spectrometer in KBr pellets. The spectra were the results of 64 scans obtained in the range of  $4000\text{--}400\text{ cm}^{-1}$  with a resolution of  $1\text{ cm}^{-1}$ .

The laser Raman spectra (LRS) were recorded on a LabRam infinity laser Raman spectrometer (JY-DILOR) equipped with an optical microscope. The laser intensity (Ar $^+$ , 514.5 nm) was reduced by various filters ( $<1$  mW) and the data were treated by Lasbpec software. The spectral resolution and the accuracy in the Raman shifts are estimated to be  $2\text{ cm}^{-1}$ . A tenth particle was examined for each sample to check its homogeneity.

Temperature programmed reduction experiments were performed on a 50 mg sample placed in a U-shaped quartz reactor (6.6 mm ID) using a heating rate of  $15^\circ\text{C min}^{-1}$  from 25 to  $900^\circ\text{C}$ . The reductive gas was a mixture of 3% H $_2$  in He (total flow rate  $50\text{ ml min}^{-1}$ ). A thermal conductivity detector analyzed the effluent gas after water trapping and permitted to quantify the hydrogen consumption.

### 2.3. Activity test

Activity tests were performed in a fixed bed reactor using 0.2 g of catalyst at atmospheric pressure and at the reaction temperature of  $700^\circ\text{C}$ . The total flow rate is of  $3.4\text{ l h}^{-1}$  with  $\text{CH}_4/\text{O}_2 = 2$ . No pre-treatment was

Table 1

Predicted and experimental Ni/Mn values as determined by atomic absorption spectroscopy.

Sample	(Ni/Mn) <sub>predicted</sub>	(Ni/Mn) <sub>experimental</sub>
CP-0.2-900	0.07	0.08
CP-0.6-900	0.25	0.27
CP-0.8-900	0.36	0.41
CP900	0.50	0.53
SG900	0.50	0.53

used. The products and reactants were analyzed by a Perkin Elmer 5500 gas chromatograph equipped with a TCD and a carboxen packed column. In all experiments, the performances of the catalysts were evaluated with the methane conversion and the product's selectivity was calculated as follows:

$$\text{CH}_4 \text{ conversion (\%)} = (\text{moles of CH}_4 \text{ converted} / \text{moles of CH}_4 \text{ in feed}) \times 100$$

$$\text{Selectivity of H}_2 \text{ (\%)} = (\text{moles of H}_2 \text{ produced} / 2 \times \text{moles of CH}_4 \text{ converted}) \times 100$$

$$\text{Selectivity of CO (\%)} = (\text{moles of CO produced} / \text{moles of CH}_4 \text{ converted}) \times 100$$

$$\text{Selectivity of CO}_2 \text{ (\%)} = (\text{moles of CO}_2 \text{ produced} / \text{moles of CH}_4 \text{ converted}) \times 100$$

## 3. Results and discussion

### 3.1. Chemical analysis

The results are tabulated in Table 1. The comparison of the predicted and experimental Ni/Mn molar ratio values shows that they are very close.

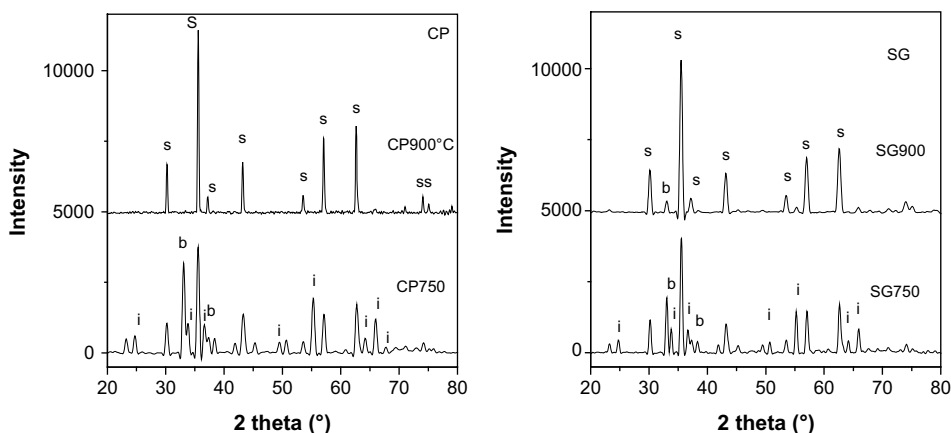


Fig. 1. XRD spectra of calcined NiMn $_2$ O $_4$  prepared by coprecipitation method (CP) and sol-gel method (SG); (s) spinel, (i) ilmenite, and (b) Mn $_2$ O $_3$  bixbyite.

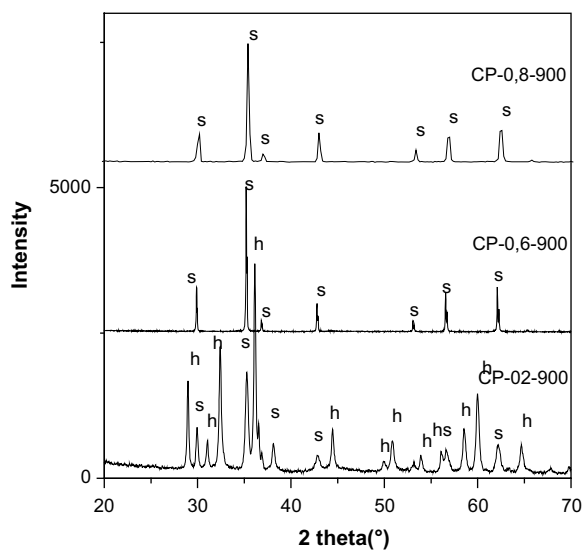


Fig. 2. XRD spectra of the series  $Ni_xMn_{3-x}O_4$  (s) spinel (h)  $Mn_3O_4$  hausmanite.

### 3.2. X-ray diffraction

XRD patterns of all solids are shown in Figs. 1 and 2.

The patterns of the solids calcined at  $900^\circ\text{C}$  show the presence of pure spinel phases for CP900, CP-0.6-900 and CP-0.8-900. Traces of  $Mn_2O_3$  were observed for the solid SG900. The diffractogram of CP-0.2-900

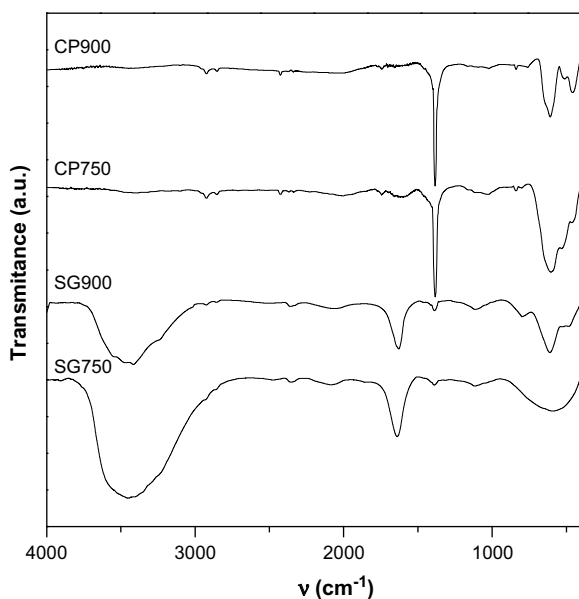


Fig. 3. FT-IR spectra of calcined  $NiMn_2O_4$  prepared by coprecipitation and sol-gel methods.

shows the presence of the spinel phase in addition to hausmanite phase:  $Mn_3O_4$ .

The solids calcined at  $750^\circ\text{C}$  show the presence of a mixture of three phases  $NiMnO_3$  (ilmenite),  $NiMn_2O_4$  (spinel) and  $Mn_2O_3$ .

### 3.3. FT-IR spectral analysis

The IR spectra are represented in Figs. 3 and 4. The FT-IR spectra of solids prepared with sol-gel method show a broad band with a maximum centered at around  $3370\text{ cm}^{-1}$ , together with a band at  $1630\text{ cm}^{-1}$ . The band at  $3370\text{ cm}^{-1}$  can be ascribed to the hydroxyl groups bonded through hydrogen bonds, whereas the band at  $1630\text{ cm}^{-1}$  corresponds to the adsorbed molecular water. These results indicate that these catalysts are hydrated and/or hydroxylated.

All the solids prepared via the coprecipitation method exhibit a relatively intense narrow band at  $1384\text{ cm}^{-1}$  which can be attributed to the nitrate vibrations. The remaining of nitrates after calcination at high temperatures is not expected. However, the presence of small quantities of sodium ions provided by the precipitation reactant ( $Na_2CO_3$ ) may stabilize a small quantity of nitrate through the formation of sodium nitrate. This salt has been already reported to be stable in air at  $850^\circ\text{C}$  [15].

In the range of  $400\text{--}1000\text{ cm}^{-1}$ , the IR bands of inorganic solids are usually assigned to the vibration of metallic ions in the crystal lattice. Two main broad

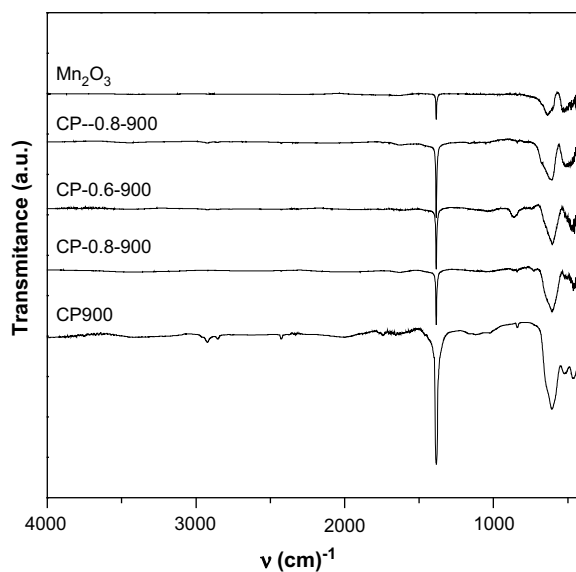


Fig. 4. FT-IR spectra of calcined  $Ni_xMn_{2-x}O_4$  ( $x=0, 0.2, 0.6, 0.8, 1$ ).

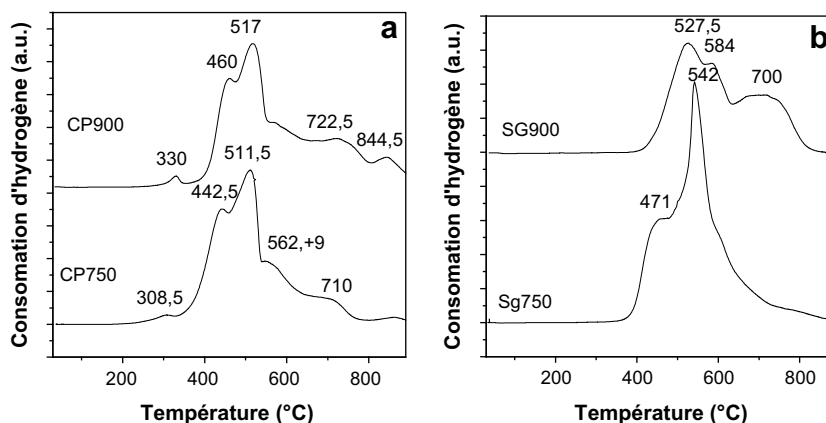


Fig. 5. Temperature programmed reduction profiles of calcined  $\text{NiMn}_2\text{O}_4$  prepared by (a) coprecipitation method and (b) sol-gel method.

metal–oxygen bands are seen in the IR spectra of normal spinels. The highest one,  $\nu_1$ , generally observed in the range of  $600\text{--}550\text{ cm}^{-1}$ , corresponds to the intrinsic stretching vibration of the metal ion at the tetrahedral site,  $\text{M}_{\text{tetra}}\text{--O}$ , whereas the  $\nu_2$  lowest band, usually observed in the range of  $450\text{--}385\text{ cm}^{-1}$ , is assigned to the octahedral metal ion stretching,  $\text{M}_{\text{octa}}\text{--O}$  [16,17]. In agreement with these statements,  $\text{Mn}_3\text{O}_4$  presents two bands at  $436\text{ cm}^{-1}$  and  $636\text{ cm}^{-1}$ . However, three bands in the range of  $450\text{--}600\text{ cm}^{-1}$  are observed in the spectra of the solids calcined at  $900\text{ }^\circ\text{C}$  which seem to indicate a partial or total inversion of the spinel  $\text{NiMn}_2\text{O}_4$ . Indeed, in the inverted spinel, octahedral sites are occupied by two types of ions which might result in the doubling of the band corresponding to the vibration of  $\text{M}_{\text{octa}}\text{--O}$ .

For the solids calcined at  $750\text{ }^\circ\text{C}$ , the appearance of more than two bands in the range of  $400\text{--}1000\text{ cm}^{-1}$  is attributed to the presence of mixed oxides formed at this temperature as shown by XRD.

### 3.4. Temperature programmed reduction

The TPR profiles for the solids CP750, CP900, SG750 and SG900 are presented in Fig. 5. For all oxides the reduction occurs practically in two main steps. The TPR curves of the coprecipitated catalysts (CP750 and CP900) show two main peaks situated at around  $443\text{--}460\text{ }^\circ\text{C}$  and  $512\text{--}517\text{ }^\circ\text{C}$ , the reduction peaks of the solid calcined at  $900\text{ }^\circ\text{C}$  are slightly shifted to higher temperatures. Additional unresolved peaks, at higher reduction temperature, are observed in the range of  $560\text{--}850\text{ }^\circ\text{C}$ .

The sol-gel solids exhibit different TPR profiles compared to the solids prepared by coprecipitation.

Moreover, the two solids show two different profiles, indeed, the solid calcined at  $750\text{ }^\circ\text{C}$  shows two reduction steps where the second one consists of one single sharp peak, meanwhile, for the solid calcined at  $900\text{ }^\circ\text{C}$ , the main reduction step is the first one in opposite to the three other solids.

The total hydrogen consumption was practically the same for the four samples and seemed not to depend on either the calcination temperature or the preparation method.

XRD analysis of the solids after TPR experiments showed that all of them consisted of a mixture of MnO and metallic nickel. These results are in agreement with the data reported in the literature [18] where it has been shown that the reduction of nickel manganites (spinel and ilmenite) occurs in two stages:



During the first stage, the major part of manganese cations are reduced to  $\text{Mn}^{2+}$ , leading to the formation of a solid solution  $\text{NiO--MnO}$ , the reduction of  $\text{Ni}^{2+}$  cations in MnO matrix occurs during the last step. According to these attributions, the reduction of nickel in our solids seems to be difficult, in that way that it occurs very slowly, giving rise to broad shoulders on the second reduction step peak; the unusual TPR profile obtained for the solid SG750 seems to indicate that the reduction of all the present nickel ends at  $700\text{ }^\circ\text{C}$ .

A small peak is observed at  $309$  and  $330\text{ }^\circ\text{C}$  on the profiles of CP750 and CP900, respectively, it can be attributed to the reduction of small free nickel oxide which could have segregated from  $\text{NiMn}_2\text{O}_4$  and  $\text{NiMnO}_3$ . The reduction of NiO has already been reported to occur in the range of  $307\text{--}370\text{ }^\circ\text{C}$  [19].

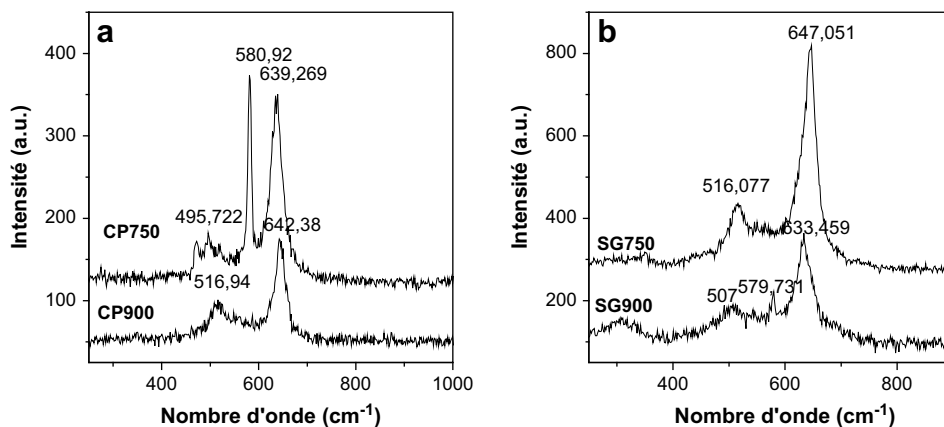


Fig. 6. Raman spectra of calcined  $\text{NiMn}_2\text{O}_4$  prepared by (a) coprecipitation method and (b) sol-gel method.

### 3.5. Raman spectroscopy analysis

Raman spectra are given in Fig. 6. CP900 and SG900 spectra exhibited two distinct bands, a weak band at about  $516\text{ cm}^{-1}$  and a stronger one at about  $645\text{ cm}^{-1}$ .

In spinel oxides and in other manganese oxides energies of  $600\text{--}650\text{ cm}^{-1}$  are characteristic of vibrations involving motion of oxygens inside the octahedral unit  $\text{MnO}_6$  [20]. The broadening of this peak in the direction of lower energies corresponds to a spinel with disordered cationic occupation (inverted spinel) [21]. The second peak, centered at around  $516\text{ cm}^{-1}$  has already been observed and has been considered as an  $F_{2g}$  mode related to  $\text{M-O}$  in tetrahedral environment [21].

For SG750 and CP750, the same two bands are preserved and a supplementary band situated at about  $580\text{ cm}^{-1}$  appeared. This Raman feature is assigned as an  $A_{1g}$  mode for regular  $\text{Mn}^{\text{IV}}\text{O}_6$  octahedra [20]. This band might, then, correspond to the manganese in the ilmenite structure as this band was absent from the Raman spectra of the solids calcined at  $900\text{ }^\circ\text{C}$ , this band is more intense in the solid prepared via the coprecipitation method which indicates that the ilmenite is more important in this solid than in the solid prepared via sol-gel method.

### 3.6. Catalyst testing

In the catalytic experiments, the catalyst is heated from ambient temperature to  $700\text{ }^\circ\text{C}$  under reaction mixture. The first analysis of the effluent gases is performed when the reaction temperature reaches  $700\text{ }^\circ\text{C}$ , the methane conversion is then very low and increases as the reaction time increases as shown in Fig. 7. The methane conversion, the products'

selectivities measured at the steady state and the thermodynamic selectivities are shown in Fig. 8.

The catalysts CP900 and SG900 displayed high and similar activities towards the partial oxidation of methane characterized by a  $\text{CH}_4$  conversion of about  $\sim 80\%$ .

Meanwhile, the solids CP750 and SG750 showed different behaviors, indeed, the solid prepared with coprecipitation method showed a methane conversion of  $51\%$  whereas the sample prepared via the sol-gel method presented a very poor activity (about  $1\%$  of  $\text{CH}_4$  converted).

Further examination of Fig. 8 let us to remark that the three active catalysts showed good selectivities

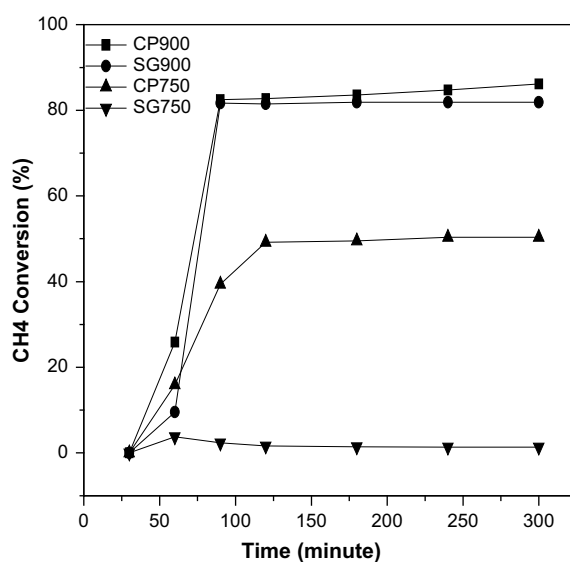


Fig. 7. Influence of time on stream on the methane conversion at  $700\text{ }^\circ\text{C}$ , S.V.:  $52900\text{ l kg}^{-1}\text{ h}^{-1}$ .



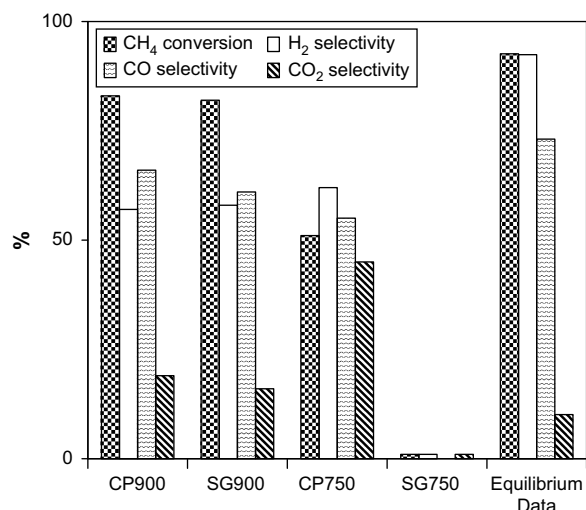


Fig. 8. Methane conversion, CO, H<sub>2</sub> and CO<sub>2</sub> selectivities at the steady state. Reaction temperature: 700 °C, S.V.: 52 900 l kg<sup>-1</sup> h<sup>-1</sup>.

towards CO and H<sub>2</sub> and that the solid CP750 leads to a high CO<sub>2</sub> selectivity. This fact may be related to the presence of the ilmenite phase (NiMnO<sub>3</sub>) which has been already proved to have excellent catalytic activity in complete hydrocarbon oxidation attributed to the manganese present in its higher oxidation state.

In order to understand the lack of catalytic activity in the case of SG750, we compared the XRD patterns obtained with the used solids (shown in Fig. 9). We can see that the used SG750 consisted, practically, of a mixture of MnO and metallic nickel which indicated that the solid undergoes deep reduction under the reaction conditions. This is consistent with the exceptional reduction behavior of this solid already observed in TPR measurements. In the same time, the XRD

Table 2

Effect of the composition of the catalysts on the conversion of CH<sub>4</sub>.

X	Conversion (%)	Iso-conversion temperature (°C)
0.2	78	850
0.6	82.8	800
0.8	79	750
1	82.7	700

patterns of the used active catalyst (e.g. CP750) showed that only a part of nickel is present as metallic phase with a size particle of 27.12 nm whereas the size particle of metallic nickel in the case of SG750 is about 5.29 μm. In the light of these observations, we propose that the inactivity of the solid SG750 is due to the sintering of the active phase and the high activity of CP750 is the consequence of the good dispersion of nickel particles.

The effect of nickel content on the catalytic activity is summarized in Table 2. We have found out that the catalysts corresponding to compositions Ni<sub>x</sub>Mn<sub>2-x</sub>O<sub>y</sub> (x < 1) exhibited very low methane conversion at 700 °C. In Table 2, we are giving the temperature at which a methane conversion of about 80% had been achieved. It appears that the decrease in nickel content caused the increase in the iso-conversion reaction temperature. This observation is in agreement with the fact that nickel is considered as the active species in POM.

#### 4. Conclusion

NiMn<sub>2</sub>O<sub>4</sub> was prepared by sol–gel and coprecipitation methods, a pure phase was obtained after calcination at 900 °C. FT-IR and Raman techniques illustrated that the synthesized spinels were inverted.

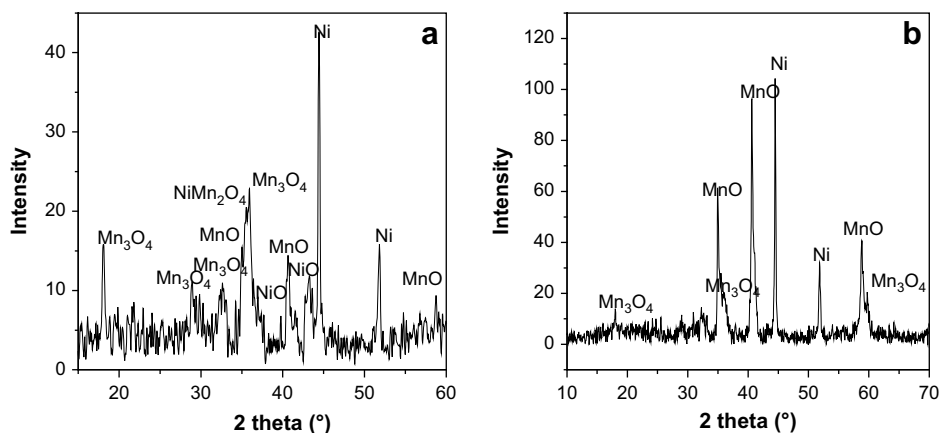


Fig. 9. XRD patterns of catalysts after methane partial oxidation (a) CP750, (b) SG750.

The calcination at 750 °C led to the formation of NiMnO<sub>3</sub> and NiMn<sub>2</sub>O<sub>4</sub> mixture. A pure spinel was also obtained at 900 °C with the sub-stoichiometric solids Ni<sub>0.6</sub>Mn<sub>2.4</sub>O<sub>4</sub> and Ni<sub>0.8</sub>Mn<sub>2.2</sub>O<sub>4</sub>.

The spinel NiMn<sub>2</sub>O<sub>4</sub> was found to be active in the reaction of the partial oxidation of methane. The catalysts calcined at 900 °C present a higher methane conversion; the reason can be the stability of the structure which led to good dispersion of nickel species. Indeed, the presence of the oxidized nickel limited the growth of the particles probably by the formation of interaction between metallic nickel out of the structure and the nickel oxide of the structure.

The catalytic activity of the ilmenite nickel–manganese in the complete oxidation of methane can be explained having in mind that, in the ilmenite structure, manganese ions are stabilized in a high oxidation state (Mn<sup>4+</sup>). Evidently, for nickel–manganese oxide catalysts, Mn<sup>4+</sup> ions were responsible for the complete oxidation reaction.

## References

- [1] M.A. Pena, J.P. Gomez, J.L.G. Fierro, *Appl. Catal.*, A 144 (1996) 7.
- [2] Y. Lu, J. Xue, C. Yu, Y. Liu, S. Shen, *Appl. Catal.*, A 174 (1998) 121.
- [3] A.M. O'Connor, J.R.H. Ross, *Catal. Today* 46 (1998) 203.
- [4] K. Otsuka, Y. Wang, E. Sunada, I. Yamanaka, *J. Catal.* 175 (1998) 152.
- [5] P.M. Yamiainen, X. Chu, L.D. Schmidt, *J. Catal.* 146 (1994) 1.
- [6] L.D. Schmidt, M. Huff, *Catal. Today* 21 (1994) 443.
- [7] J.T. Richardson, S.A. Paripatyadar, *Appl. Catal.* 61 (1990) 293.
- [8] A.M. Gaddalla, M.E. Sommer, *Chem. Eng. Sci.* 44 (1989) 2825.
- [9] T. Utaka, S.A. Al-Drees, J. Ueda, Y. Iwasa, T. Takeguchi, R. Kikuchi, K. Eguchi, *Appl. Catal.*, A 247 (2003).
- [10] H. Provendier, C. Petit, C. Estournès, S. Libs, A. Kiennemann, *Appl. Catal.* 180 (1999) 163.
- [11] Y. Chen, W. Zhou, Z. Shao, N. Xu, *Catal. Commun.* 9 (2008) 1418.
- [12] J. Papavasiliou, G. Avgouroupoulos, T. Ionnides, *J. Catal.* 251 (2007) 7.
- [13] D. Mehandjiev, E. Zhecheva, G. Ivanov, R. Ioncheva, *Appl. Catal.* 167 (1998) 277.
- [14] J.C. Varges, S. Libs, A. Roger, A. Kiennemann, *Catal. Today* 107–108 (2005) 417.
- [15] P. Pascal, *Nouveau Traité de Chimie Minérale*, Masson Cie, Paris, vol. 1, 1966. p. 637.
- [16] S. Hafner, *Z. Kristallogr.* 115 (1961) 331.
- [17] R.D. Waldron, *Phys. Rev.* 99 (1955) 172.
- [18] C. Laberty, P. Alphonse, A. Dupart, A. Rousset, *Thermochim. Acta* 306 (1997) 51.
- [19] A.M. Diskin, R.H. Cunningham, R.M. Ormerod, *Catal. Today* 46 (1998) 147.
- [20] D.H. Park, S.T. Lim, S.J. Hwang, J.H. Choy, J.H. Choi, J. Choo, *J. Power Sources* 159 (2006) 1346.
- [21] L.M. Alavasi, P. Galineto, M.C. Mozzati, C.B. Azzouni, G. Flor, *Phys. Chem. Chem. Phys.* 4 (2002) 3876.